

Accepted Manuscript

Huthaifa Ahmad, Yoshihiro Nakata, Yutaka Nakamura, and Hiroshi Ishiguro, "A study on energy transfer among limbs in a legged robot locomotion," *Adaptive Behavior*, vol.26, no.6, pp.309-321, Copyright © 2018 SAGE Publications. DOI:10.1177/1059712318798733

A Study on Energy Transfer among Limbs in a Legged Robot Locomotion

Journal Title
XX(X):1-14
©The Author(s) 2016
Reprints and permission:
sagepub.co.uk/journalsPermissions.nav
DOI: 10.1177/ToBeAssigned
www.sagepub.com/



Huthaifa Ahmad¹, Yoshihiro Nakata¹, Yutaka Nakamura¹ and Hiroshi Ishiguro¹

Abstract

Realizing adaptability to environmental changes requires the robot's body to change according to the environment. From this perspective, several studies have considered variable compliant actuation to change the physical characteristics of the robot as it interacts with the environment. Robots with this ability show a variety of efficient stable motions during contact with the environment. However, having locally variable compliant parts with independent dynamics under the same body may be insufficient for achieving adaptability in diverse environments. To extend the idea of variable compliant actuation, from being used locally to the level of the entire body's dynamics, in the present study, we use an actuator network system (ANS). As an approximation of bipedal robots, we developed an eight-legged rimless wheel robot with an ANS that allows energy transfer among limbs through passive interactions among mutually interconnected air cylinders mounted on the robot's legs. We experimentally demonstrated that by using the ANS to realize energy transfer among limbs, the robot performance improved.

Keywords

Actuator network system, legged robot, locomotion, morphological computation, entire body's dynamics.

1 Introduction

For decades, researchers have focused on bipedal robots that can walk like humans (Collins (2005); McGeer (1990); Torricelli (2016)). However, it is not easy to realize a walking robot owing to the complexity of the interactions required among all the parts of the robot body to produce the required gait patterns. To overcome these difficulties, robotics researchers have been following two approaches, numerical computation and morphological computation.

Robots with bipedal locomotion following the numerical computation approach, for example, HRP-2 (Kaneko et al. (2004)) or Honda's Asimo (Hirose & Ogawa (2007)), which is considered one of the best-performing and robust humanoid robots, have demonstrated outstanding locomotion versatility. However, the walking patterns of these robots deviate considerably from those of humans, and precise models of the robot body and the environment in which the robot is embedded are required to achieve adaptability.

Robots following the morphological computation approach on the other hand (Pfeifer & Bongard (2006)), many of which are inspired from the well-designed structures of animals (Narioka (2012); Sprowitz (2013)), use the dynamic and physical characteristics of their bodies. They exploit their interaction with the environment to produce more efficient and natural behaviors. A typical example is passive dynamic walkers (PDWs) (Collins (2001); McGeer (1990); Tedrake (2004)). They exhibit an energy-efficient and natural human-looking walking gait without employing any actuator or control system and are capable of walking down a ramp simply by exploiting their dynamics (the manner in which gravity, friction, and other forces generated by the swinging of the legs and arms act

on them). Despite their efficiency, PDWs are not versatile and sensitive to external perturbation, which make them unadaptable to environmental changes.

Realizing adaptability to environmental changes requires the robot's body to change according to the environment. From this perspective, several studies have considered variable compliant actuation to change the physical characteristics of the robot as it interacts with the environment (Geyer (2006); Pratt (1995); Vanderborght (2013)). Robots with this ability show a variety of efficient stable motions during contact with the environment (Hobbelen (2008); Hosoda (2007), (2008); Huang (2013)). However, having "locally"* variable compliant parts with independent dynamics under the same body may be insufficient for achieving adaptability in diverse environments.

To extend the idea of variable compliant actuation, from being used locally to the level of the entire body's dynamics, in the present study, we use an actuator network system (ANS). ANS has been proposed in previous studies to enhance a robot's adaptability in response to environmental changes (Ryu, Nakata, Nakamura, and Ishiguro (2015), (2016)). ANS is composed of multiple actuators that are connected to each other through tubes and valves with

¹Graduate School of Engineering Science, Osaka University, Japan

Corresponding author:

Huthaifa Ahmad, Osaka University, 1-3 Machikaneyama, Toyonaka, Osaka, 560-8531, Japan.

Email: huthaifa.ahmad@irl.sys.es.osaka-u.ac.jp

*Locally variable compliant parts: are the compliant actuators that do not have a DIRECT interaction between each other.

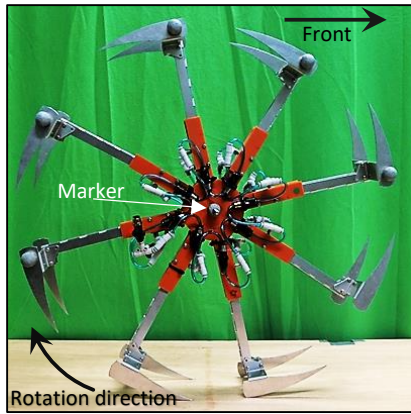


Figure 1. Eight-legged rimless wheel robot OCTANS.

fluid-mediated interaction between them. By changing the connection patterns between the actuators, the fluid flow will change the interaction between them, thus, changing the entire body's dynamics. Therefore, from a morphological point of view, the robot can change its morphology according to the environment by changing the connection patterns between its actuators. Here in the present study, ANS is used to allow energy transfer among limbs through passive interactions among mutually interconnected air cylinders mounted on a robot's legs. With two conducted experiments, we will check how the different connection patterns can be used to improve the robot's behavior based on the given situation.

To investigate the way in which energy transfer between the legs of a robot can improve its walking performance, we developed a multi-legged robot, more specifically, an eight (OCT)-legged rimless wheel robot with an ANS, as shown in figure 1. Rimless wheel robots can be considered as an approximation of bipedal robots (figure 2). In the case of such a robot, one may visually ignore the legs that are not in contact with the ground (swinging legs) and instead consider that another leg is recirculating to prepare for the next step; then the dynamics of its periodic motion relates well to the cyclic motion of bipedal robots (Asano (2012); Coleman (1997); McGeer (1990); Torricelli (2016)). By considering a rimless wheel robot as a representative of bipedal robots for the purpose of this study, we can focus on the dynamics of the entire body and its role in improving gait patterns without having to concern ourselves with other issues such as balancing and falling down.

The position of our study among other studies on robotics is shown in figure 3. As the axes indicate, the distribution of these robots is based on two parameters: a) whether the focus is on morphological computation or numerical computation and b) whether the robot has rigid or compliant legs. For example, the position of Aldebaran NAO (Gouaillier et al. (2009)) in figure 3 can be ascribed to its rigid body structure and active control of every joint angle at all times. The Delft biped robot (Collins, Ruina, Tadrake, and Wisse (2005)), by contrast, is placed on the opposite side because it employs lower levels of control and energy than other powered robots owing to the morphological contribution of its compliant hip actuation and its passive ankle. The shifted-up robots exhibit whole body dynamics.

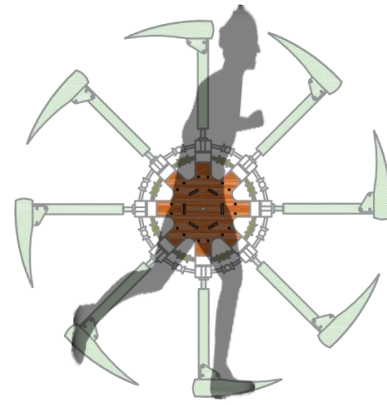


Figure 2. Schematic diagram of OCTANS.

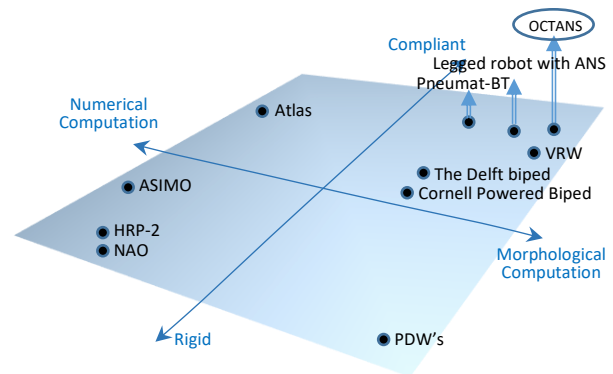


Figure 3. Research map showing the position of OCTANS with respect to other robots.

The remainder of this paper is structured as follows. Section 2 presents the structure of the robot developed herein, and explains the ANS and its connection patterns that are tested in the experiments. Section 3 explains the experimental setups, procedures of both conducted experiments, and their results. Based on the experimental results, in this section, we evaluate robot performance and discuss how the robot can realize an efficient gait pattern by using the ANS. Section 4 presents the concluding remarks.

2 Rimless wheel with actuator network system

The proposed rimless wheel robot OCTANS shown in figure 1 is constructed symmetrically with eight identical legs that are attached to the main body through eight pneumatic cylinders.

As shown in figure 4-a, each leg has a semicircular foot, and all eight legs together form a circle of 52 cm diameter when all of the robot's legs are set at their half-advanced lengths as shown in figure 4-c. This circular shape of the foot helps the robot to achieve a smoother movement by reducing the collision impact forces against the ground. A linear motion guide unit comprising two plates elongated from the robot's main body, as shown in figure 4-a guides the robot's legs, allows it to move linearly along the cylinder axis, and prevents it from rotating during the robot's locomotion.

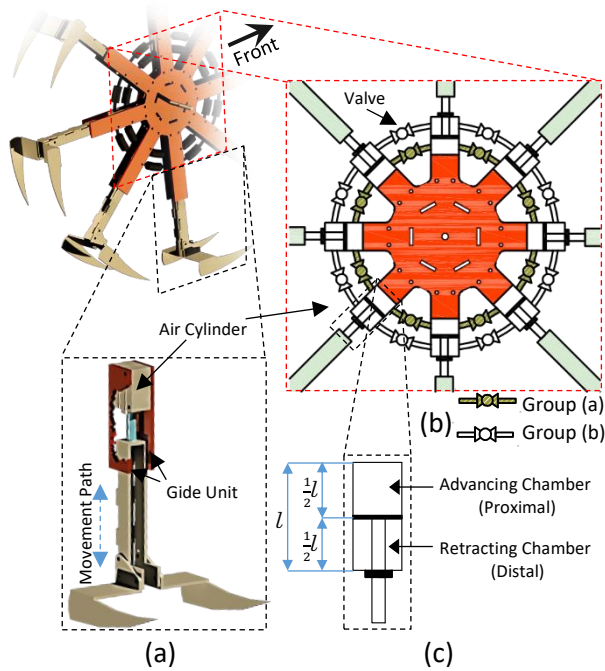


Figure 4. (a) Structure of each leg; (b) Valve system of the ANS; (c) Cylinder's initial condition, with piston set at its half advanced-length.

2.1 Valve system of ANS

ANS was introduced in previous researches to enhance and improve robots' adaptability (Ryu et al. (2015), (2016)). The central idea underlying ANS lies in how a network of mutually interconnected cylinders exhibit different behaviors based on how these cylinders are connected to each other.

As shown in figure 4-b, a valve system of two groups (a) and (b) is built using 16 "hand"[†] valves to form the ANS of our robot OCTANS. This valve system connects the robot's legs with each other. Group (a) connects the advancing (proximal) chambers of all cylinders, while group (b) connects the retracting (distal) chambers of all cylinders. With different sets of opened/ closed valves, different connection patterns among the robot's legs can be realized, and with these different connection patterns, different robot behaviors can be achieved.

2.2 Mechanism of energy transfer among limbs

In the present study, we expect to find a connection pattern that will allow energy transfer among the robot's legs to realize a walking behavior similar to the sequence of motion shown in figure 5. A connection pattern where actuators implemented to the successive legs are mutually connected (e.g., condition 2 mentioned in section 2.3). Just before placing the robot on the ground to start its locomotion, as in figure 5-1, all robot legs are made to have the same advancing lengths by setting all the cylinders to their mid stroke. Once the fore leg (L2) hits the ground, as in figure 5-2, it will fully retract, causing the air in the attached cylinder to be transmitted to the successive rear cylinder attached to leg (L1); at this moment, (L1) will expand, kick the ground, and push the robot forward in the rolling direction to prepare for

the next step (figure 5-3). During the robot's locomotion, the same process will be repeated along the way on every step the robot takes, helping to keep it moving.

In addition to the energy transfer among the limbs of the robot during locomotion by using the ANS, as shown in figure 5, if our expectations are right, the robot will push the ground with its rear leg just before it enters the swing phase. This behavior is similar to human walking during the terminal stance and pre-swing phases, where the foot applies a posteriorly directed force to the ground to propel the body forward and prepare it for the next step (Neumann (2009)).

2.3 Connection patterns

To test our hypotheses, the robot's behaviors were compared under three different connection patterns, as shown in figure 6. Under condition 1, all 16 valves of both groups of the ANS are kept open, ensuring that the advancing chambers of all cylinders are connected to each other, and the retracting chambers of all cylinders are connected to each other. In this condition, the movement of one leg will affect the behavior of all other legs, for example, in an ideal case (ignoring the friction and pressure loss during air transmission), if one of the legs is retracted by 10 mm, each of the remaining seven legs will advance by 1.43 mm.

Under condition 2, eight valves are opened, four from each group, and connected alternatively, as shown in figure 6-b. In this condition, the advancing chamber of cylinder i will be connected to the advancing chamber of cylinder $i+1$, while the retracting chamber of cylinder i will be connected to the retracting chamber of cylinder $i-1$. Once the leg attached to cylinder i hits the ground and fully retracts, the high pressure generated in the advancing chamber of cylinder i will transmit the air to the advancing chamber of cylinder $i+1$, which will cause the leg attached to it to expand. At the same time, the low pressure generated in the retracting chamber of cylinder i will suck the air from the retracting chamber of cylinder $i-1$, causing the leg attached to it to expand as well. In other words, here in this condition there are two groups of legs, odd-numbered legs and even-numbered legs as shown in figure 6-b. The retraction of one leg for a certain distance, will cause the other three legs of the same group to retract the same distance, while the other four legs from the second group will advance the same distance. For example, in the ideal case, if one of the odd-numbered legs retracted by 10 mm, each of the odd-numbered legs will retract by 10 mm as well, while each of the even-numbered legs will advance by 10 mm.

Under condition 3, all 16 valves are left closed, as shown in figure 6-c. There is no interaction among the robot's legs, and the air sealed inside the cylinders will make each leg to behave as if it is attached to an independent pneumatic spring. Note that this condition corresponds to standard PDWs with compliant legs.

[†]Hand valve: is a hand-operated valve, with a quarter turn movement lever to manually change the (open/ close) status of the valve.

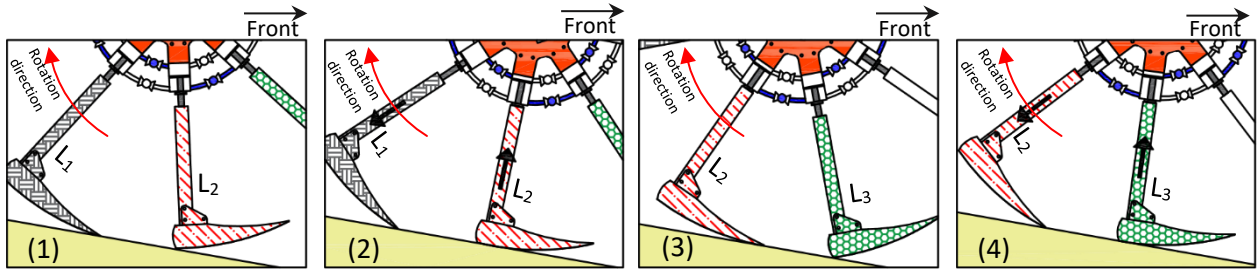


Figure 5. Mechanism of energy transfer among robot limbs during locomotion.

3 Experiments:

Two experiments were conducted to investigate the effect of the three previously mentioned connection patterns on the robot's behavior in terms of the driving force required to start robot locomotion, which is represented by the slope angle, and the efficiency of the robot, which represented by the distance traveled.

3.1 Experimental Setups:

Given that OCTANS is fully passive and gravity is the only power source for its locomotion, both experiments herein were conducted by placing the robot on an inclined board with a variable slope angle controlled using a screw jack, as shown in figures 7-a and b. Before starting the trials of the two experiments, the following three preparation steps were performed on the robot:

1. Pressurizing the ANS with air by using an air compressor.
2. Adjusting the pressure in ANS groups (a) and (b) to the appropriate values to set all legs at mid stroke.
3. Changing the connection patterns manually to one of the three previously mentioned conditions and fixing it during the robot's locomotion.

3.2 Traveling Distance Experiment [TD]

In this experiment we investigate the effect of the three previously mentioned connection patterns on the distance traveled by the robot after leaving the inclined board. The experiment was conducted with two slope angles, $\Theta = 10^\circ$ and $\Theta = 15^\circ$, and the ANS pressurized to 0.10 MPaG. Ten trials were conducted for each connection pattern. In each trial, and after going through the experimental setups mentioned in section 3.1, the following procedures were performed:

1. The robot was placed on an inclined board with a fixed slope angle ($\Theta = 10^\circ$, $\Theta = 15^\circ$).
2. The robot was passively rolled down the inclined board, as shown in figure 7.
3. The distance traveled and the number of steps walked by the robot after leaving the inclined board were measured.

To track the robot's movement, a motion capture system (V120: Trio tracking system, NaturalPoint, Inc. DBA OptiTrack) was used. The robot position was defined by a reflective marker attached to the center point of the robot, as shown in figure 1.

3.2.1 Results: For the ten trials conducted for each connection pattern, the average distance traveled in addition to the number of steps walked by the robot are listed in table 1. Regardless the value of the slope angle, as the

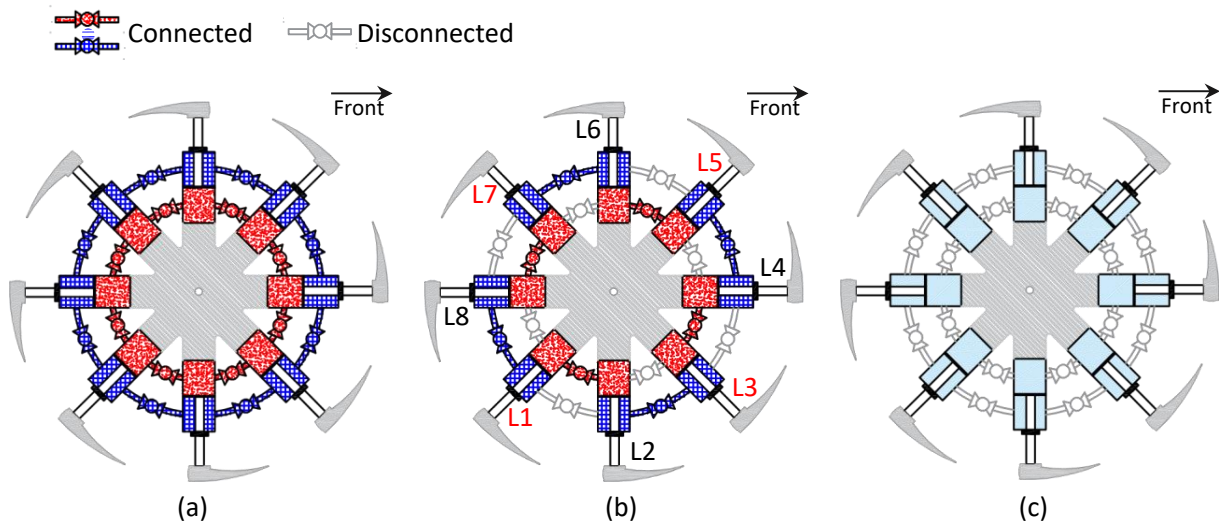


Figure 6. Connection patterns used in experiments. (a) Condition 1: all valves of the ANS are kept open to ensure mutual interaction among all legs. (b) Condition 2: eight valves of the ANS are opened, four from each group allowing to create two groups of legs, odd- and even-numbered legs. (c) Condition 3: no interaction among the legs since all valves of the ANS are left closed.

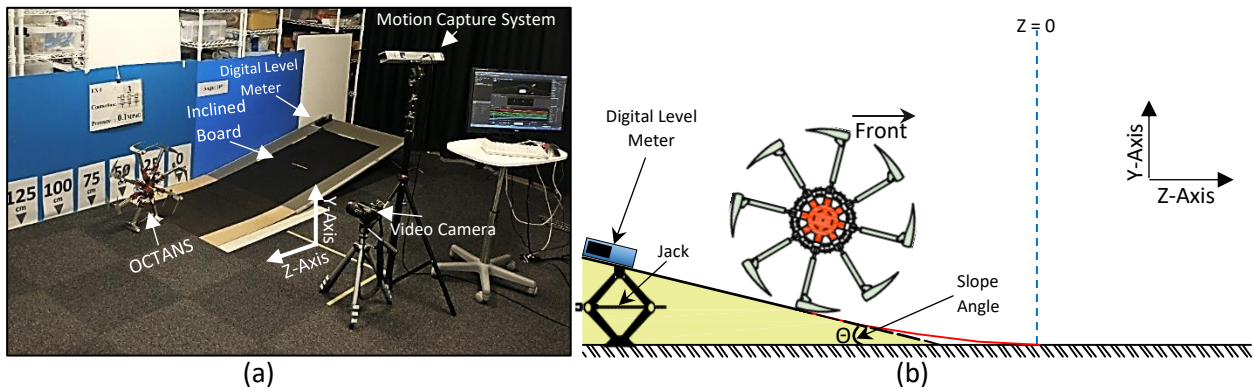


Figure 7. (a) Experimental environment; (b) Schematic of experimental setup.

results show, the robot with independent spring-like legs under condition 3 was able to walk a greater number of steps after leaving the inclined board compared to the other two connection patterns that use the ANS to mutually interconnect the robot's legs with each other; therefore, under this condition, the robot traveled a significantly ($p < 0.001$) longer distance compared to those under the other two conditions according to a t-test performed with 18 degrees of freedom, as shown in figure 8. The robot relatively travelled a longer distance under condition 2 compared to condition 1, although it was not a significant difference ($p = 0.006 > 0.001$).

The results of the TD experimental trials are summarized in figures 9-a and b, which compare the distance traveled and the speed of the robot under the three conditions and two different slope angles of $\Theta = 10^\circ$ and $\Theta = 15^\circ$. The black line represents one of the commonly occurring behaviors across the 10 trials under each condition. After the robot reaches its maximum speed at the end of the inclined board (at $z = 0$) and leaves it to move on level ground, as shown in figure 9-b, under condition 3, the robot decelerates at a lower rate compared to that under the other two conditions, helping it retain its energy and travel a longer distance.

As an example, time-series photographs of OCTANS during locomotion (figure 10) show the motion sequence of the robot under the three connection patterns and slope angle of $\Theta = 15^\circ$, as denoted by the black lines in figure 9.

Under the three conditions, figure 11 shows the changes happened to the lengths of the robot's legs during the first three steps of its locomotion (the period from the moment leg L2 hits the ground until leg L5 hits the ground as shown in figure 11-d). With no interaction between the legs under condition 3, a robot's leg partially retracts during its contact with the ground before it returns to its initial length once it enters the swing phase as shown in figure 11-c. Under condition 1, as shown in figure 11-a, with all legs being mutually connected with each other, once one of the legs hits the ground, it fully retracts to affect the lengths of the other legs. A clear interaction between the robot's legs is happening under condition 2 as shown in figure 11-b. Once a leg hits the ground as the figure shows, it fully retracts, causing the successive rear leg to relatively fully expand and pushing the robot forward in the rolling direction, to realize a behavior similar to the expected sequence of motion shown in figure 5.

Table 1. Average of distance traveled [m] and number of steps walked by robot after leaving inclined board \pm S.D at slope angles of $\Theta = 10^\circ$ and $\Theta = 15^\circ$.

		Condition 1	Condition 2	Condition 3
$\Theta = 10^\circ$	Traveled Distance	1.00 ± 0.23	1.11 ± 0.15	1.64 ± 0.13
	Number of Steps	5.20 ± 1.03	5.70 ± 0.67	8.40 ± 0.84
$\Theta = 15^\circ$	Traveled Distance	1.21 ± 0.19	1.43 ± 0.18	1.97 ± 0.13
	Number of Steps	6.10 ± 0.86	7.30 ± 0.82	9.90 ± 0.57

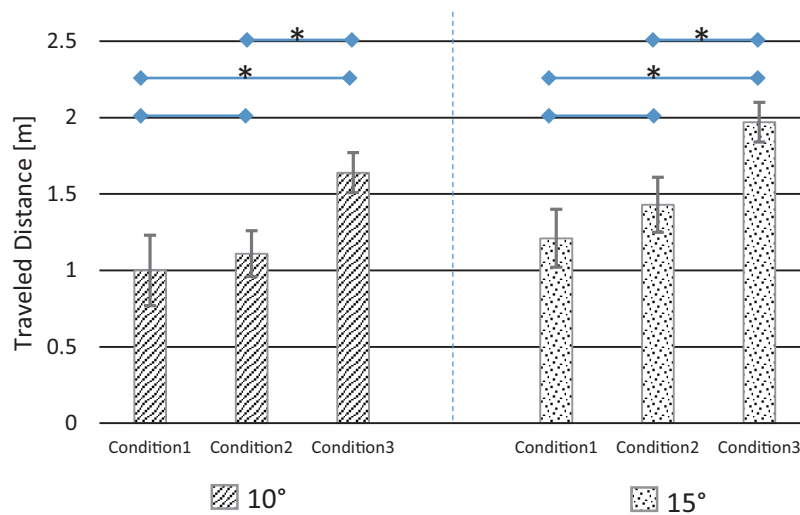


Figure 8. Average distance traveled \pm S.D. at slope angles of $\Theta = 10^\circ$ and $\Theta = 15^\circ$. (*) indicates $p < 0.001$.

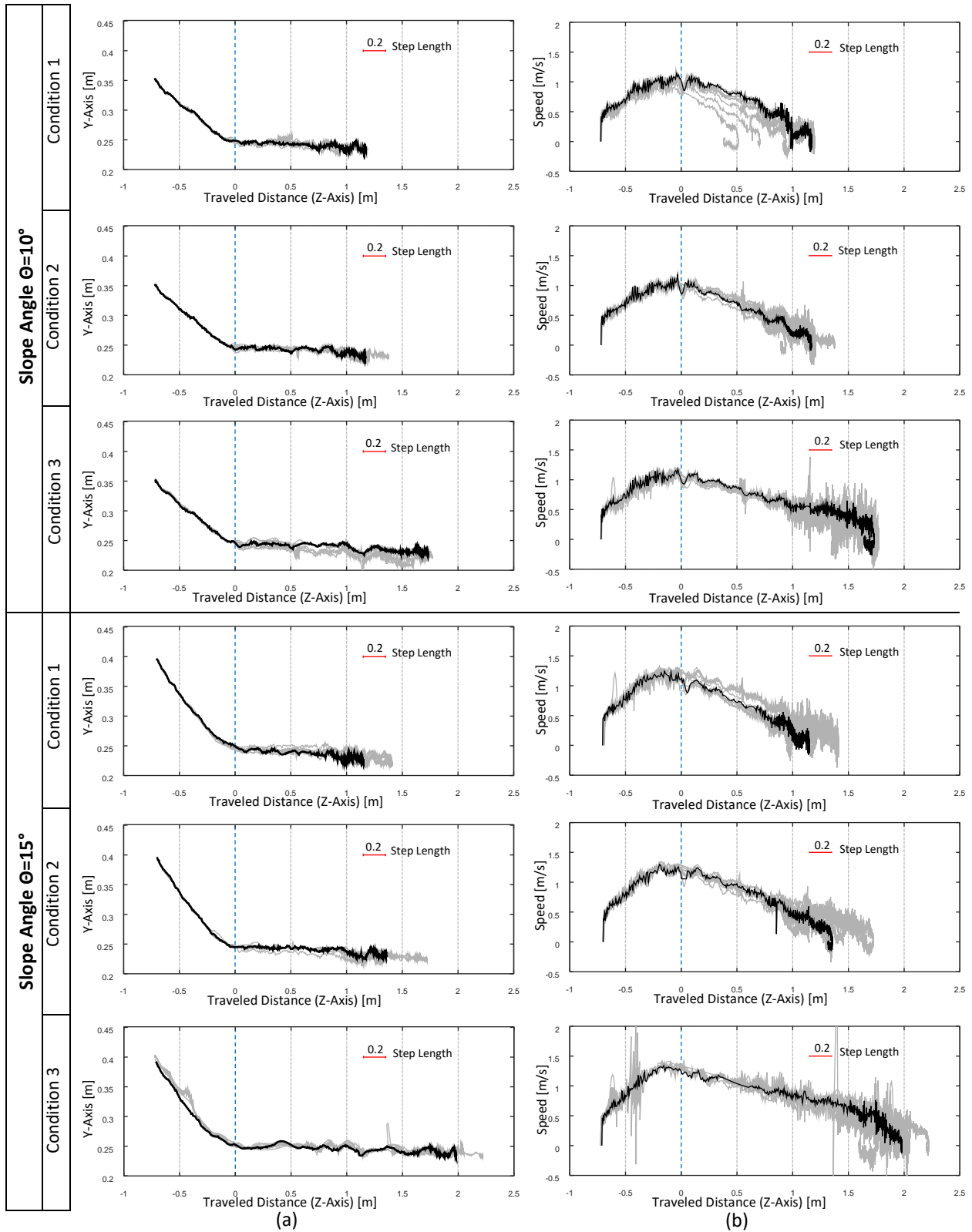


Figure 9. Comparison of distance traveled and robot speed under three conditions and two different slope angles of 10° and 15° . (a) Distance traveled and (b) speed. The black line represents a typical behavior (Median) across 10 trials under each condition. The dashed line ($z = 0$), represents the end of the slope and the beginning of horizontal ground.

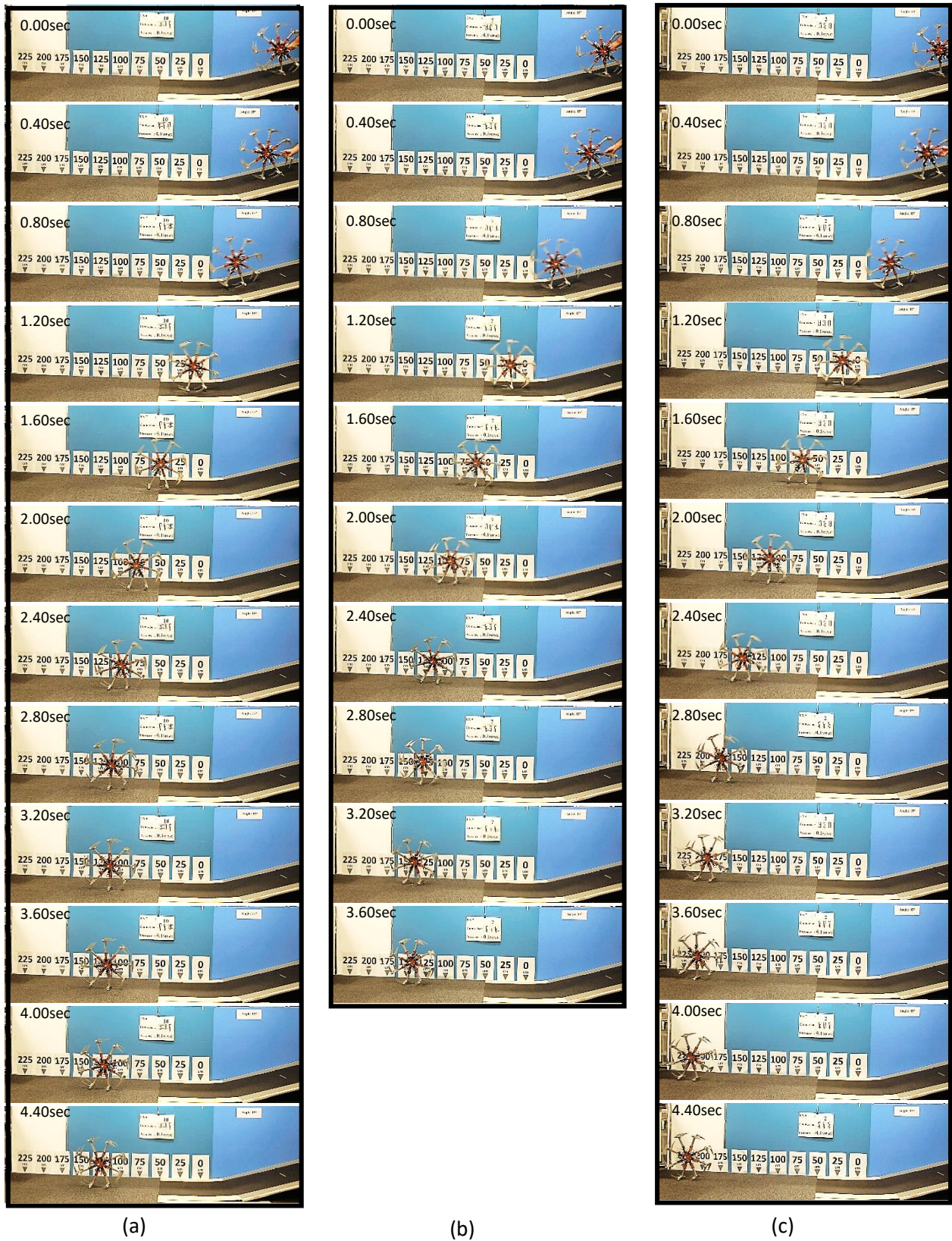


Figure 10. (a), (b), and (c) show time-series photographs of OCTANS during locomotion, representing the black lines of figure 9 on board with a slope angle of 15° under conditions 1, 2, and 3, respectively. The interval between the two pictures is 0.40 s.

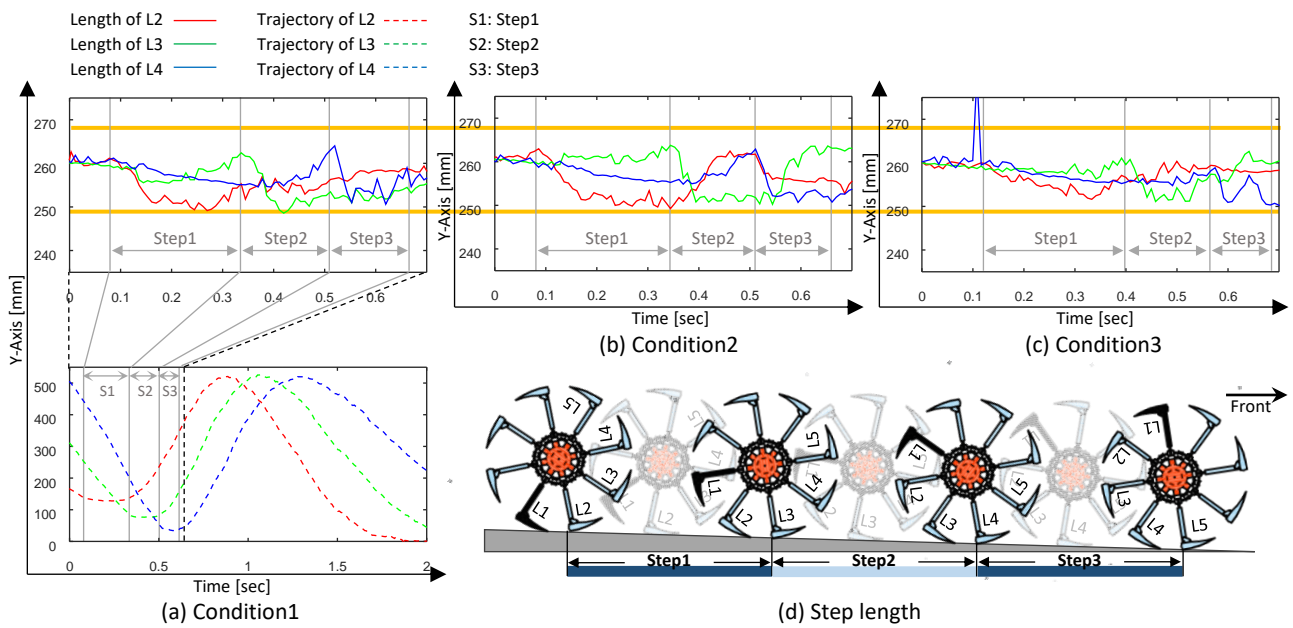


Figure 11. (a), (b) and (c) show the changes in length happening to the robot’s legs L2, L3 and L4 during the first three steps of the robot’s locomotion, under the conditions 1, 2 and 3 respectively. The lower part of figure (a), shows the trajectories of the legs L2, L3 and L4 during the first two seconds (almost one cycle) of the robot’s locomotion. As shown in figure (d), a step is defined by the period between the moment a leg hits the ground until the next following leg hits the ground. The two horizontal orange lines indicate the shortest/ longest possible lengths due to the hardware limitations.

3.3 Driving Force Experiment [DF]

In this experiment, we investigated the effect of the three previously mentioned connection patterns on the driving force required by the robot to start locomotion. To this end, we measured the minimum slope angle of the inclined board that caused the robot to start moving. This minimum slope angle was called the Motion Initiation Slope Angle (MISA). The experiment was conducted with two different pressure values for the ANS, 0.10 MPaG and 0.20 MPaG. For each connection pattern, 10 trials were conducted. In each trial, after going through the experimental setups mentioned in section 3.1, the following procedures were performed:

1. The robot was placed on a horizontally laid board with the slope angle of $\Theta = 0^\circ$.
2. The slope angle was increased gradually by using a screw jack, as shown in figure 7, until the robot started moving.
3. The MISA was measured using a digital level meter (DI-230M) that measures the exact angle of the inclined board with respect to the horizontal ground with a resolution of 0.05° .

3.3.1 Results: Table 2 presents a comparison of the average MISA over 10 trials for each connection pattern and two different values of air pressure (0.10 MPaG and 0.20 MPaG) inside the ANS. Regardless the value of the air pressure inside the ANS, as the results show, the robot with mutually interconnected legs under conditions 1 and 2, which realizes energy transfer among the robot's legs during locomotion, needed smaller MISA for the robot to start moving compared to the robot under condition 3, which has independent spring-like legs. In other words, under conditions 1 and 2, the robot needed lower driving force to start its locomotion compared to that under condition 3.

The results of the DF experimental trials are summarized in figure 12. For the two pressure values (0.10 MPaG and 0.20 MPaG) inside the ANS, the MISAs of the robot under the three conditions are significantly different ($p < 0.001$) from one another, as indicated by the results of a t-test with 18 degrees of freedom.

As an example, time-series photographs of OCTANS with 0.10 MPaG pressurized ANS during locomotion, as in figure 13, show one of the commonly occurring MISA across the 10 trials of the robot conducted under conditions 1, 2, and 3 after increasing the slope angle gradually until the robot started moving.

3.4 Discussion

For the DF experiment, it is reasonable to find that under conditions 1 and 2, the robot with ANS requires lower driving force to start locomotion compared to that in condition 3, in which the robot has independent spring-like legs. The underlying reason is that because the ANS allows for energy transfer among legs, especially under condition 2, where the air transmission between legs as the fore leg hits the ground, causes the successive rear leg to relatively fully expand while the fore leg is fully retracted as shown in figure 5-2 and figure 11-b. In response, the robot's center of mass is raised and pushed forward. The robot then falls in the rotation direction with potential energy being converted

Table 2. Average of MISA [deg] ± S.D. for three connection patterns at pressure values of 0.10 MPaG and 0.20 MPaG.

	Condition 1	Condition 2	Condition 3
0.10 MPaG	3.49 ± 0.52	1.61 ± 0.22	6.00 ± 0.58
0.20 MPaG	3.23 ± 0.56	1.79 ± 0.40	5.73 ± 1.12

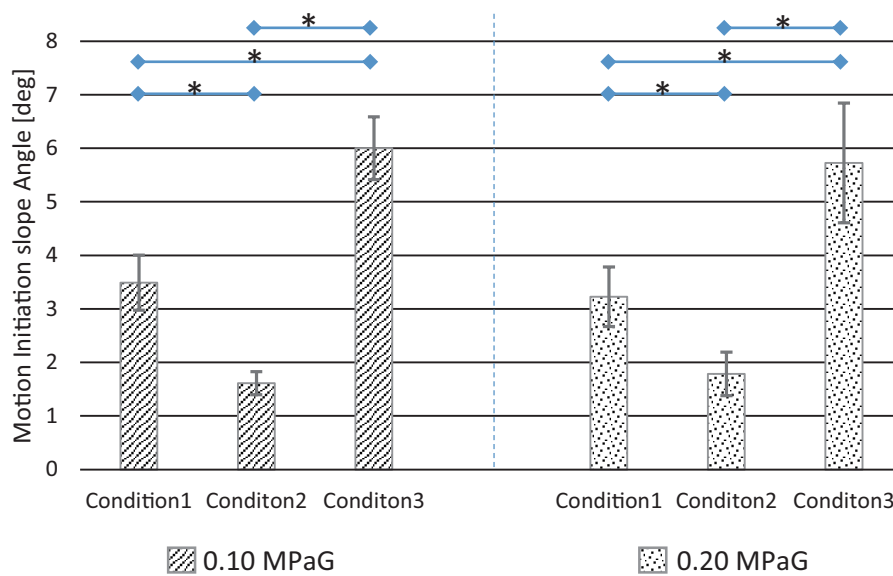


Figure 12. Average of MISA [deg] ± S.D. for three connection patterns at pressure values of 0.10 MPaG and 0.20 MPaG. (*) indicates $p < 0.001$.



Figure 13. Time-series photographs of OCTANS with 0.10 MPaG pressurized ANS during locomotion, showing one of the commonly occurring MISAs across 10 trials under (a) condition 1, (b) condition 2, and (c) condition 3, after increasing the slope angle gradually until the robot started moving. The interval between two pictures is 0.47 s.

to kinetic energy. It is worth noting that these changes in potential and kinetic energies during walking are very similar to the changes that occur in a human during walking (Blazevich (2007)).

In the TD experiment, we can see that under conditions 1 and 2, the robot travels shorter distances compared to that under condition 3, although they all started their locomotion from the same height with same potential energy (mgh). The robot's behavior in this case can be explained by the dissipation of energy that takes place as a result of the friction between the legs and their guide units during retraction and expansion of the robot's legs, as well as because of the pressure loss due to the friction between the tubes and air during the transmission of air from one leg to another. Therefore, by increasing the air pressure in the ANS, the interaction among the robot's legs can be improved and by enhancing the design of both the legs and their guide units, this behavioral limitation can be mitigated, and the robot would be more energy efficient.

With a closer look to the results of both TD and DF experiments, we can notice that the robot under condition 2 seems to have a better behavior in all cases compared to the robot under condition 1. From the TD experiment at slope angle of $\Theta = 15^\circ$, the robot under condition 2 has travelled longer distance compared to condition 1, although it was not a significant difference ($p = 0.006$) based on the performed t-test. From the DF experiment, the robot under condition 2 needed smaller MISA to start moving compared to condition 1 with a significant difference ($p < 0.001$) as indicated by the performed t-test with 18 degrees of freedom. This superiority in performance in case of condition 2 over condition 1 can be related to the way the robot's legs are interacting with each other under each condition. If a leg retracted a certain distance under condition 2, in the ideal case, it would cause all other legs to retract/ advance the same distance. On the other hand, if one of the legs under condition 1 retracted a certain distance, in the ideal case, each of the remaining seven legs would advance by one-seventh that distance.

The connection pattern of the robot was changed manually before starting each trial by switching (open/ close) the hand valves of the ANS that mutually connect the robot's legs with each other. Thus during the robot's locomotion, it retained the predetermined connection pattern without having the ability to change it. As can be inferred from the experiment results, the connection pattern that is suitable for starting the robot's gait differs from the connection pattern that is best for the stationary gait phase. Based on these observations and to improve the robot's performance to generate an efficient gait through all locomotion phases, in future work, we will replace the manually actuated hand valves with electronically actuated ones. This would allow the robot to automatically change the connection pattern of its ANS during locomotion based on the given situation. Moreover, to ensure movement continuity on a level ground, a simple actuation mechanism, such as a rotary motor, will be installed.

4 Conclusion

In the present work, we reported the development of an eight-legged rimless wheel robot OCTANS that uses

passive interactions among the air cylinders attached to its legs to transfer energy from one leg to another. With a focus on the role of ANS in transferring energy among the robot's legs, two experiments were conducted to test the effects of different connection patterns on the robot's walking behavior. In the Traveling Distance experiment, we investigated the distance traveled by the robot after leaving an inclined board as an indication of the robot's efficiency. The results showed that the robot with independent spring-like legs was able to travel a significantly longer distance compared to the robot with mutually interconnected legs. In the Driving Force experiment, we investigated the Motion Initiation Slope Angle needed to trigger the robot's movement as an indication of the minimum driving force required for the robot to start its locomotion. The results showed that the robot with mutually interconnected legs, which realizes energy transfer among its legs during locomotion, needed a smaller MISA to initiate motion compared to the robot with independent spring-like legs.

From the results of both experiments, the robot's demands differ based on the given situation. i.e. Based on the DF experiment, the robot needed a connection pattern that realizes a mutual interaction between its legs to start locomotion with lower driving force, while for a stationary gait pattern, as can be inferred from the TD experiment, the robot required a different connection pattern that prevents any interaction among its legs to reduce energy dissipation during locomotion, and as a result, the robot traveled longer distance. Therefore, in the future, by enabling the robot to proactively choose an adequate connection pattern and autonomously change it during locomotion, the robot can realize adaptability to any given situation and develop an efficient gait pattern through all locomotion phases.

5 Acknowledgements

This work was partially supported by Japan Society for the Promotion of Science Grants-in-Aid for Scientific Research Grant number JP26700026.

References

- Fumihiko Asano and Junji Kawamoto. (2012). Passive Dynamic Walking of Viscoelastic-legged Rimless Wheel. IEEE International Conference on Robotics and Automation
- Anthony J. Blazevich. (2007). Sports Biomechanics: The Basics: Optimising Human Performance. A&C Black.
- Coleman, M. J., Chatterjee, A., & Ruina, A. (1997). Motions of a rimless spoked wheel: a simple three-dimensional system with impacts. *Dynamics and Stability of Systems* 12:139159.
- S. H. Collins, M. Wisse, & A. Ruina. (2001). A three-dimensional passivedynamic walking robot with two legs and knees. *International Journal of Robotics Research*, vol. 20, no. 7, pp. 607615.
- Collins, A. Ruina, R. Tedrake, & M. Wisse. (2005). Efficient Bipedal Robots Based on Passive-Dynamic Walkers. *Science*, vol. 307, no. 5712, pp. 1082-1085.
- H. Geyer, A. Seyfarth, & R. Blickhan. (2006). Compliant leg behaviour explains basic dynamics of walking and running. *Proceedings of Royal Society of London B* 273, 14712954.

- D. Gouaillier, V. Hugel, P. Blazevic, C. Kilner, J. Monceaux, P. Lafourcade, et al. (2009). Mechatronic design of NAO humanoid. IEEE International Conference on Robotics and Automation- Kobe-Japan
- Hirose M & Ogawa K. (2007). Honda humanoid robots development Phil. Trans. A365 119
- Hobbelen D, De Boer T, & Wisse M. (2008). System overview of bipedal robots flame and TULip: tailor-made for limit cycle walking. IEEE/RSJ Int. Conf. on Intelligent Robots and Systems, IROS pp 248691
- Koh Hosoda & Kenichi Narioka. (2007) Synergistic 3D Limit Cycle Walking of an Anthropomorphic Biped Robot. Proceedings of the IEEE/RSJ International Conference on Intelligent Robots and Systems San Diego, CA, USA. '
- Hosoda K, Takuma T, Nakamoto A, & Hayashi S. (2008). Biped robot design powered by antagonistic pneumatic actuators for multi-modal locomotion Robot. Auton. Syst. 56 4653.
- Huang Y, Vanderborght B, VanHamR, Wang Q, VanDamme M, XieG & LefeberD. (2013). Step length and velocity control of a dynamic bipedal walking robot with adaptable compliant joints. IEEE/ASME Trans. Mechatronics 18 598611
- K. Kaneko, F. Kanehiro, S. Kajita, H. Hirukawa, T. Kawasaki, M. Hirata, et al. (2004). Humanoid robot HRP-2 Robotics and Automation. Proceedings. ICRA '04. 2004 IEEE International Conference on-New Orleans, LA, USA
- T. McGeer. (1990). Passive dynamic walking. Int. J. of Robotics Research, vol. 9, no. 2, pp. 6282, 1990.
- K. Narioka, A. Rosendo, A. Sprowitz, & K. Hosoda. (2012). Development of a Minimalistic Pneumatic Quadruped Robot for Fast Locomotion. in Proceedings of the IEEE International Conference on Robotics and Biomimetics, pp. 307-311.
- D. Neumann. (2009). kinesiology of the musculoskeletal system foundation for rehabilitation. second edition page.656. Mosby.
- R. Pfeifer & J. Bongard. (2006). How the Body Shapes the Way We Think A New View of Intelligence. The MIT Press.
- G. A. Pratt & M. M. Williamson. (1995). Series Elastic Actuators. Proceedings of IEEE International Conference on Intelligent Robots and Systems.
- Hideyuki Ryu, Yoshihiro Nakata, Yutaka Nakamura, & Hiroshi Ishiguro. (2015). Adaptive Whole-body Dynamics: An Actuator Network System for Orchestrating Multi-joint Movements. ROBOTICS AND AUTOMATION MAGAZINE, VOL. 14, NO. 8.
- Hideyuki Ryu, Yoshihiro Nakata, Yutaka Nakamura, & Hiroshi Ishiguro. (2016). Adaptive Locomotion by Two Types of Legged Robots with an Actuator Network System. IEEE/RSJ International Conference on Intelligent Robots and Systems (IROS).
- A. Sprowitz, A. Tuleu, M. Vespignani, M. Ajallooeian, E. Badri, & A. J. Ijspeert. (2013). Towards Dynamic Trot Gait Locomotion: Design, Control, and Experiments with Cheetah-cub, a Compliant Quadruped Robot. The International Journal of Robotics Research, vol.32, no.8, pp.932950.
- R. Tedrake, T. W. Zhang, M. Fong, & H. S. Seung. (2004). Actuating a Simple 3D Passive Dynamic Walker. Proc. IEEE Int. Conf. Robotics Automation (IEEE, New Orleans, LA).
- Diego Torricelli, Jose Gonzalez, Maarten Weckx, Ren Jimnez-Fabin, Bram Vanderborght, Massimo Sartori, et al. (2016). Human-like compliant locomotion: state of the art of robotic implementations. IOP publishing- Bioinspir. Biomim. 11 (2016) 051002
- B. Vanderborght, A. Albu-Schaeffer, A. Bicchi, E. Burdet, D.G. Caldwell, R. Carloni, et al. (2013). Variable impedance actuators: a review. Robot. Auton. Syst. 61 160114